

Electronic Supplementary Information For:

**Drastic performance improvement of indoor organic
photovoltaics using novel laminated homojunction hole-
transport layer**

Tae Hyuk Kim^a, Justin Scott Neu^b, Sung Hyun Kim^a, Muhammad Ahsan Saeed^a, Wei You^{*b} & Jae Won Shim^{*a}

Equivalent circuit model

The performance of the OPVs is often described with a single-diode equivalent circuit model, and

including one current source and two parasitic resistances, a shunt resistance (R_p) and a series resistance (R_s) under illumination. The R_p is related to the leakage current, recombination, *etc.*, and the R_s is originated from the resistive components of the device such as resistance of electrodes and bulk resistance of photoactive layers.

By using the Shockley Eq. ^{1,2}, the circuit model under illumination can be formulated, the J_{sc} and the V_{oc} can be expressed as follows,

$$J_{sc} = -\frac{1}{1 + \frac{R_s}{R_p}} \left[J_{ph} - J_0 \left(\exp\left(\frac{|V_{sc}| R_s A}{nkT}\right) - 1 \right) \right] \quad (1)$$

$$V_{oc} = \frac{kT}{q} \ln \left\{ 1 + \frac{J_{ph}}{J_0} \left(1 - \frac{V_{oc}}{J_{ph} R_p A} \right) \right\} \approx \frac{kT}{q} \ln \left\{ 1 + \frac{J_{ph}}{J_0} \right\} \quad (2)$$

, where J_{ph} is the photo-current density, J_0 is the reverse saturation current density, n is the ideality factor, q is the elementary charge number (1.602×10^{-19} C), k is the Boltzmann constant (8.617×10^{-5} eV/K), T is temperature, and A is the area of the photoactive region. Also, when R_p

$\gg R_s$ and $J_{ph} = J_{sc}$, Eq. (2) can be written as $V_{oc} \approx \frac{kT}{q} \ln \left\{ 1 + \frac{J_{ph}}{J_0} \right\}$, which seems to be independent of R_s and R_p . The $R_s A$ and $R_p A$ values were extracted from the inverse slope of the J - V characteristics under illumination in the range of 0.96 – 1.0 V and near 0 V (close to the J_{sc} point), respectively. The FF ($J_{max} \times V_{max} / J_{sc} \times V_{oc}$) can be shown as a function of the normalized V_{oc} ($v_{oc} = eV_{oc}/nkT$), normalized R_s ($r_s = R_s/R_{CH}$), and normalized R_p ($r_p = R_p/R_{CH}$), where the characteristic resistance (R_{CH}) is defined as $R_{CH} = V_{oc}/(J_{sc}A)$. The equation for the ideal FF₀ of the OPVs is expressed as follows:

$$FF_0 = \frac{v_{oc} - \ln(v_{oc} + 0.72)}{v_{oc} + 1} \quad (3)$$

where, $R_s = 0$ and $R_p = \infty$. However, owing to the parasitic resistance effects, the real FF value should deviate from the ideal FF₀, and thus, semi-empirical expressions with the parasitic effects are shown below:

$$FF_S = FF_0 (1 - 1.1r_s) + 0.19r_s^2, \quad (0 \leq r_s \leq 0.4, 1/r_p = 0) \quad (4)$$

and,

$$FF_{SP} = FF_0 \left\{ 1 - \frac{(v_{oc} + 0.7)FF_S}{v_{oc} r_p} \right\}, \quad (0 \leq r_s + 1/r_p \leq 0.4) \quad (5)$$

$$V_{oc} = \frac{E_{gap}}{q} - \frac{kT}{q} \ln \left\{ \frac{(1 - P_D)\gamma N_C^2}{P_D G} \right\} \quad (6)$$

where E_{gap} is the energy difference between the HOMO-donor and LUMO-acceptor, q is the elementary charge, k is the Boltzmann constant, T is temperature in Kelvin, P_D is the dissociation

probability of the electron (e)-hole (h) pairs, γ is the Langevin recombination constant, N_C is the effective density of states, and G is the generation rate of bound e-h pairs.

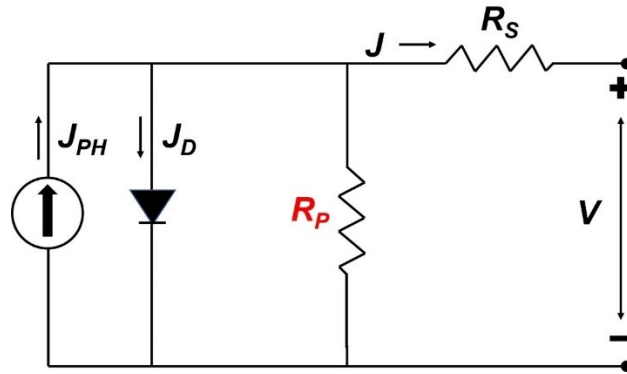


Fig. S1. Parasitic resistance effects based on the single-diode equivalent circuit model.

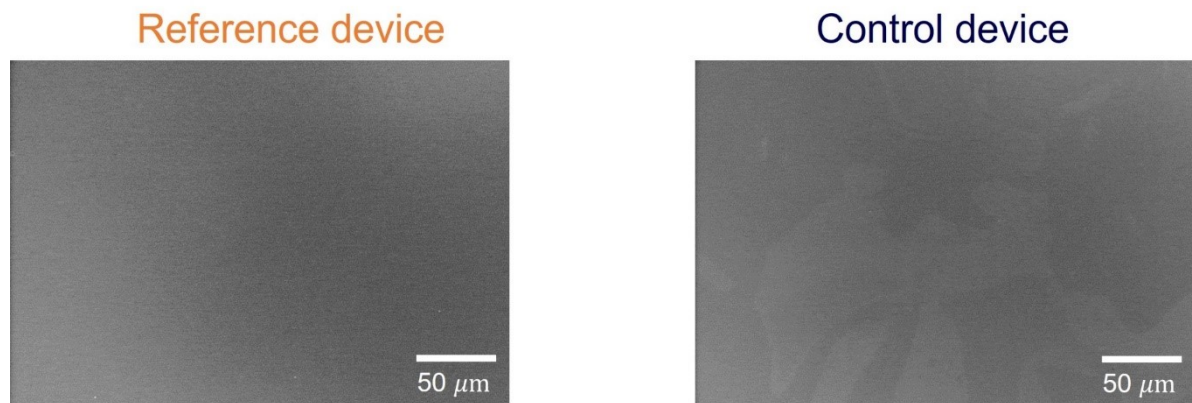


Fig. S2. The presence of PTQ10 is verified based on the top-down view of each SEM image.

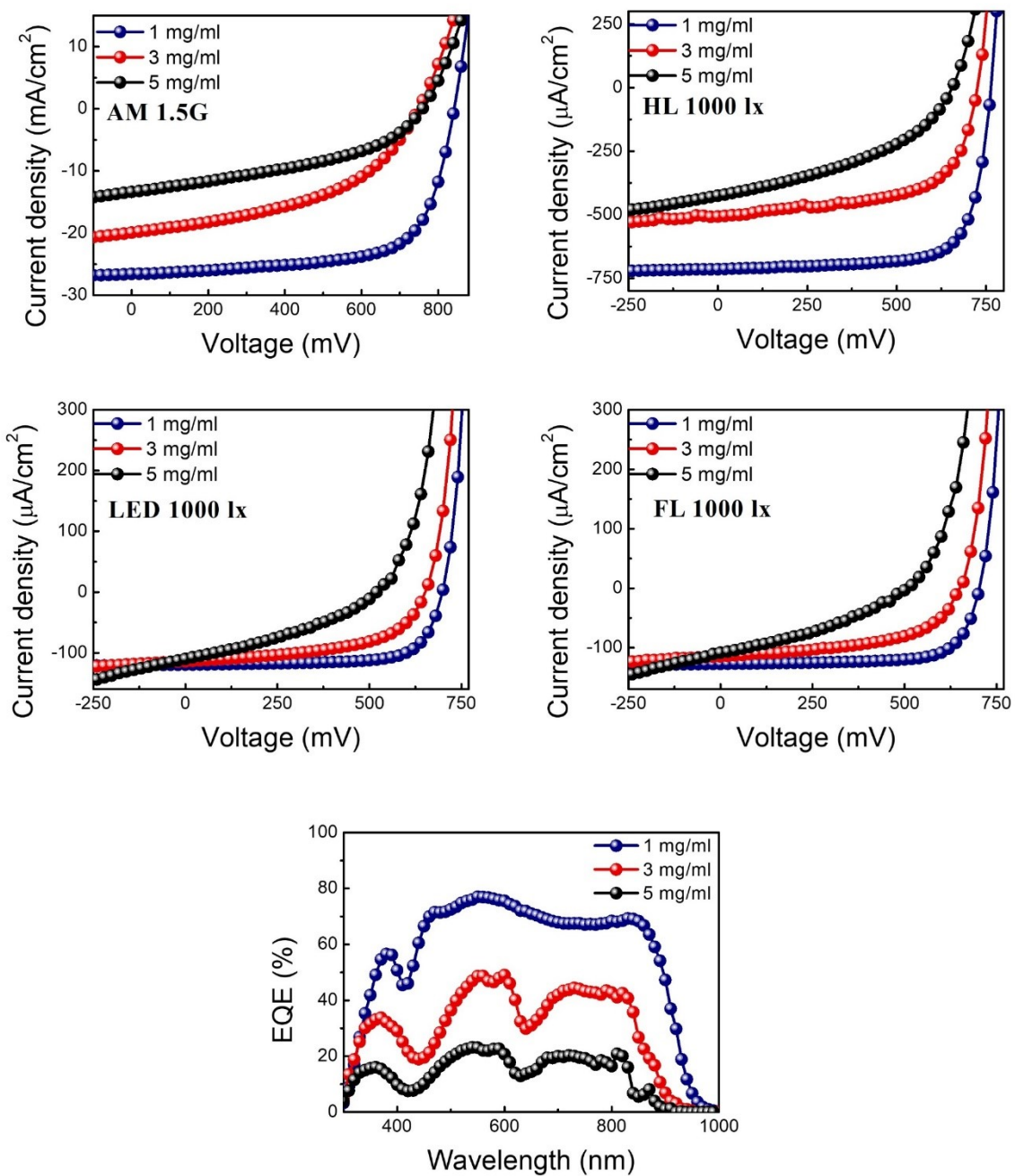


Fig. S3. Photovoltaic performance of the PTQ10-based OPV with different concentration.

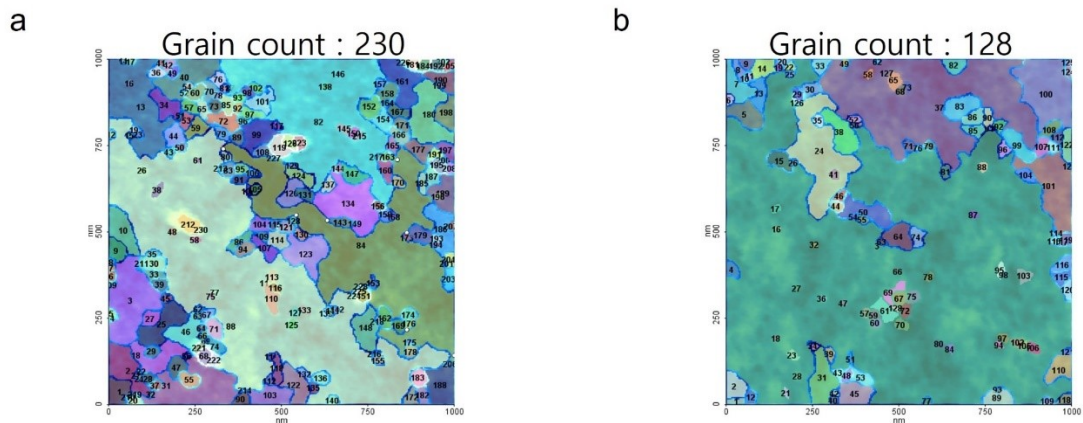


Fig. S4. 2D AFM grain-count drawings (a) PTQ10:Y6 and (b) PTQ10:Y6/PTQ10

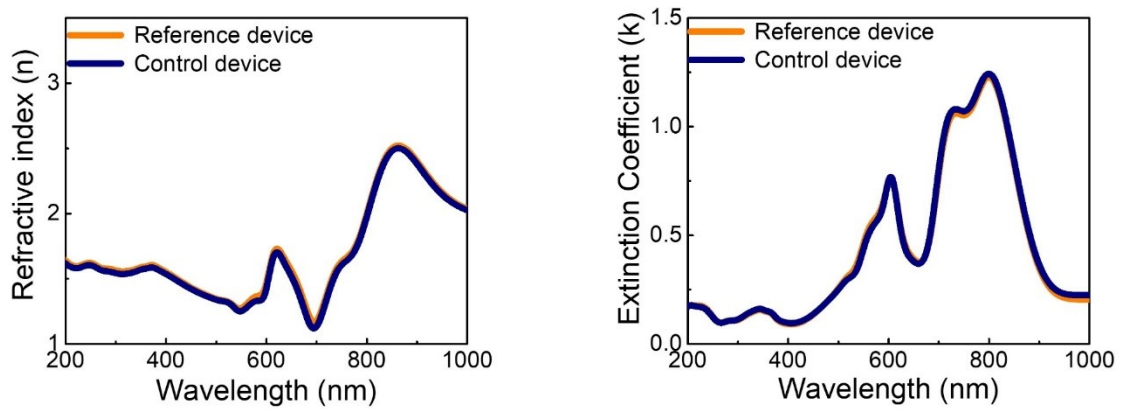


Fig. S5. Complex refractive index (n , k) of PTQ10 transport layers used for the finite-difference time-domain simulations.

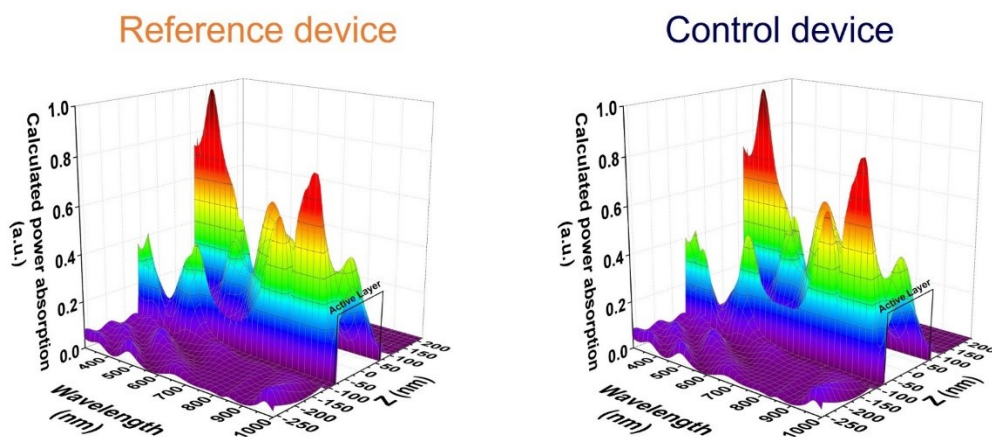


Fig. S6. Power-absorption profile of multicomponent photoactive blends obtained by the finite-difference time-domain method.

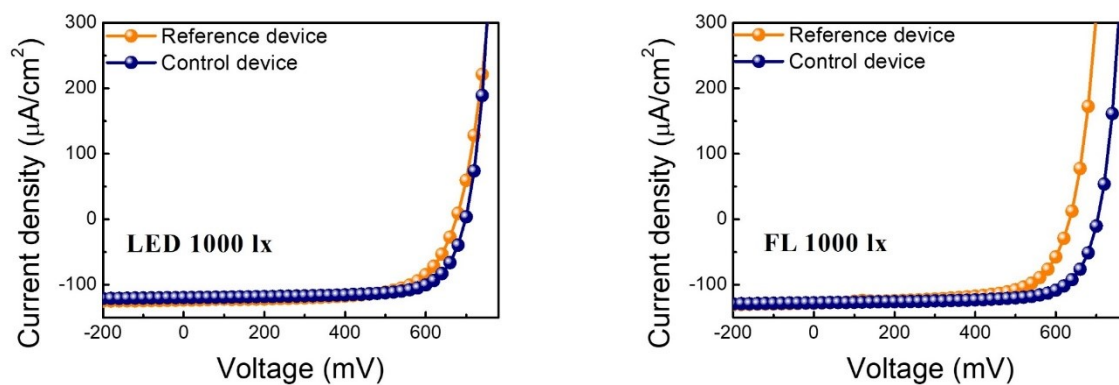


Fig. S7. Photovoltaic performance of Reference and Control devices under indoor (LED 1000 lx; FL 1000 lx) luminance.

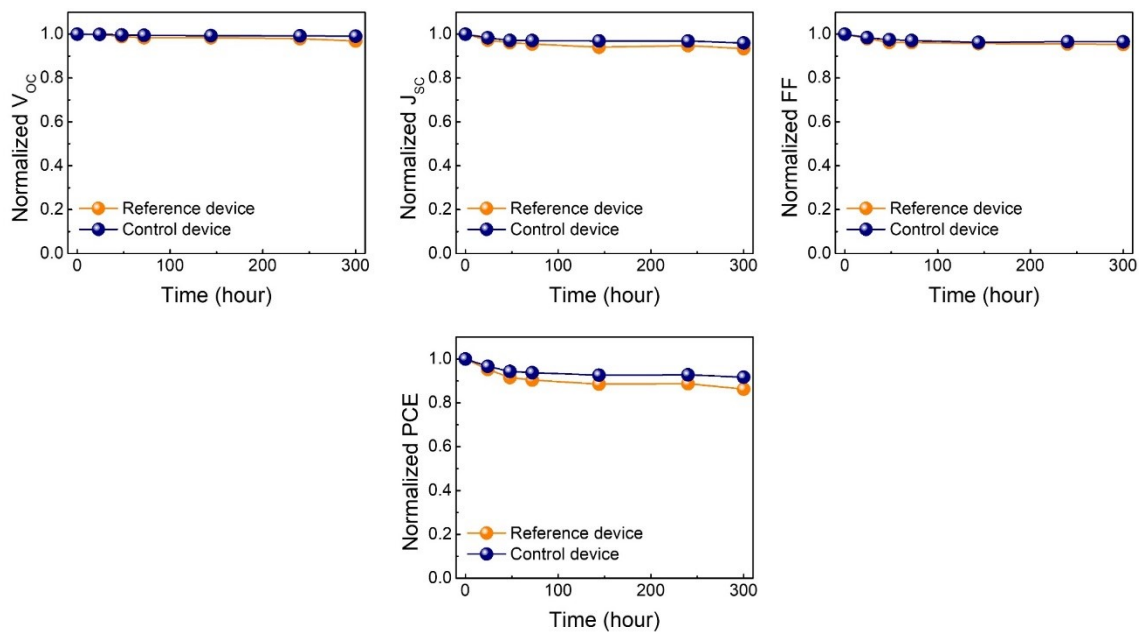


Fig. S8. Device stability of Reference and Control devices.

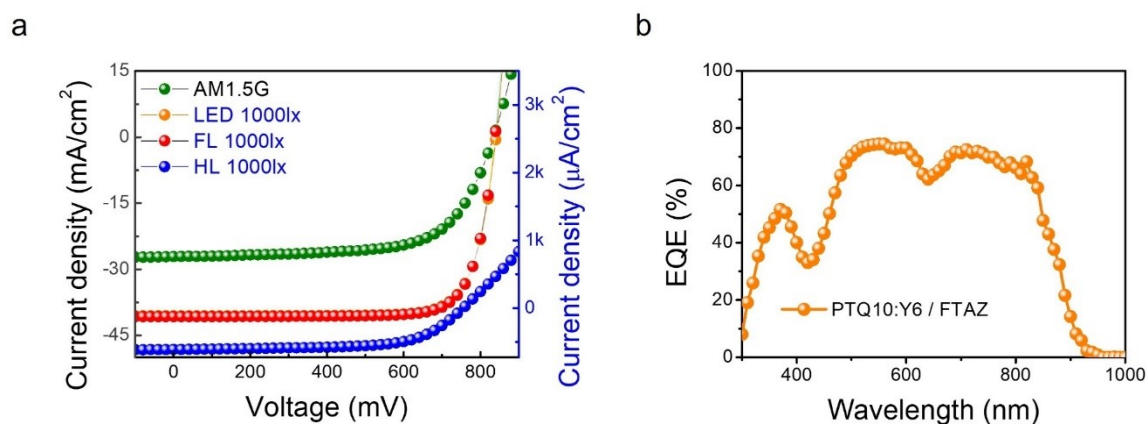


Fig. S9. (a) Photovoltaic performance of FTAZ-based device under outdoor and indoor (LED 1000 lx; FL 1000 lx; HL 1000 lx) luminance, (b) EQE spectra.

Table S1. Photovoltaic performance parameter of the PTQ10-based OPV with different concentration.

| Light source | PTQ10 concentration (mg/ml) | V_{oc} (mV) | J_{sc} | | FF (%) | PCE (%) |
|--|-----------------------------|---------------|------------------------------|------------------------------------|----------------|----------------|
| | | | (1-sun: mA/cm ²) | (Indoor: μ A/cm ²) | | |
| 1-sun (100mW/cm ²) | 1 | 841 \pm 11 | 26.9 \pm 1.2 | | 66.8 \pm 1.1 | 15.1 \pm 0.5 |
| | 3 | 740 \pm 8 | 19.7 \pm 0.3 | | 45.1 \pm 1.5 | 6.6 \pm 0.4 |
| | 5 | 774 \pm 18 | 15.8 \pm 2.7 | | 41.7 \pm 1.7 | 5.1 \pm 0.8 |
| LED 1000 lx (0.23mW/cm ²) | 1 | 698 \pm 2 | 119.5 \pm 0.3 | | 72.8 \pm 0.1 | 26.4 \pm 0.1 |
| | 3 | 651 \pm 3 | 113.9 \pm 0.1 | | 54.8 \pm 0.1 | 17.7 \pm 0.1 |
| | 5 | 516 \pm 5 | 110.2 \pm 0.1 | | 34.9 \pm 0.4 | 8.6 \pm 0.1 |
| FL 1000 lx (0.27mW/cm ²) | 1 | 703 \pm 2 | 126.0 \pm 3.1 | | 72.9 \pm 0.3 | 23.9 \pm 0.6 |
| | 3 | 649 \pm 2 | 114.1 \pm 0.9 | | 54.0 \pm 0.1 | 14.8 \pm 0.2 |
| | 5 | 60 \pm 7 | 104.9 \pm 0.7 | | 23.8 \pm 0.6 | 0.6 \pm 0.1 |
| HL 1000 lx (7.0mW/cm ²) | 1 | 785 \pm 8 | 685.2 \pm 2.5 | | 74.0 \pm 0.3 | 5.7 \pm 0.2 |
| | 3 | 726 \pm 2 | 507.5 \pm 0.2 | | 61.4 \pm 0.1 | 3.2 \pm 0.1 |
| | 5 | 191 \pm 4 | 538.6 \pm 3.2 | | 26.5 \pm 0.5 | 0.4 \pm 0.1 |

Table S2. In finite-difference time-domain (FDTD) simulation, the ideal current density of Reference and Control devices under halogen (HL) lighting.

| Sample name | $J_{ph,ideal}$ | |
|------------------|--------------------------------------|---------------------------------------|
| | HL 500lx (μ A/cm ²) | HL 1000lx (μ A/cm ²) |
| Reference device | 659.114 | 973.944 |
| Control device | 647.352 | 956.809 |

Table S3. Photovoltaic performance parameter of the PTQ10-based OPV under indoor (LED 1000lx; FL 1000lx) luminance.

| Light source | Structure | V_{oc} | J_{sc} | FF | PCE |
|--------------|-----------|----------|----------|----|-----|
|--------------|-----------|----------|----------|----|-----|

| | | (mV) | ($\mu\text{A}/\text{cm}^2$) | (%) | (%) |
|--|------------------|-------------|-------------------------------|----------------|----------------|
| LED 1000 lx (0.23mW/cm ²) | Reference device | 675 \pm 2 | 123.4 \pm 0.1 | 68.3 \pm 0.3 | 23.7 \pm 0.1 |
| | Control device | 698 \pm 2 | 119.5 \pm 0.3 | 72.8 \pm 0.1 | 26.4 \pm 0.1 |
| FL 1000 lx (0.27mW/cm ²) | Reference device | 680 \pm 2 | 124.2 \pm 2.0 | 67.5 \pm 0.4 | 21.1 \pm 0.4 |
| | Control device | 703 \pm 2 | 126.0 \pm 3.1 | 72.9 \pm 0.3 | 23.9 \pm 0.6 |

Table S4. Photovoltaic performance parameter of the FTAZ-based OPV under outdoor and indoor (LED 1000 lx; FL 1000 lx; HL 1000 lx) luminance.

| Light source | V_{oc} (mV) | J_{sc} (1-sun: mA/cm ²) (Indoor: $\mu\text{A}/\text{cm}^2$) | FF (%) | PCE (%) |
|---|------------------|--|----------------|----------------|
| 1-sun (100 mW/cm ²) | 833 \pm 2 | 27.1 \pm 0.1 | 66.6 \pm 0.2 | 15.0 \pm 0.1 |
| LED 1000 lx (0.23 mW/cm ²) | 688 \pm 4 | 120.7 \pm 4.3 | 69.0 \pm 0.8 | 24.9 \pm 0.3 |
| FL 1000 lx (0.27 mW/cm ²) | 692 \pm 2 | 125.4 \pm 2.2 | 68.5 \pm 0.9 | 22.0 \pm 0.2 |
| HL 1000 lx (7.0 mW/cm ²) | 756 \pm 3 | 650.5 \pm 15.4 | 67.6 \pm 0.1 | 4.7 \pm 0.1 |

References

- 1 J. S. Goo, J. H. Lee, S. C. Shin, J. S. Park and J. W. Shim, *J. Mater. Chem. A*, 2018, **6**, 23464–23472.
- 2 B. Kippelen and J. L. Brédas, *Energy Environ. Sci.*, 2009, **2**, 251–261.